The Power of Hard-Sphere Models: Explaining Side-Chain Dihedral Angle Distributions of Thr and Val

Alice Qinhua Zhou,[†¶] Corey S. O'Hern,[§¶] and Lynne Regan[†‡¶]

[†]Department of Molecular Biophysics and Biochemistry, [‡]Department of Chemistry, and [§]Departments of Mechanical Engineering and Materials Science and Physics, [¶]Integrated Graduate Program in Physical and Engineering Biology, Yale University, New Haven, Connecticut

Supporting Material

Figure S1

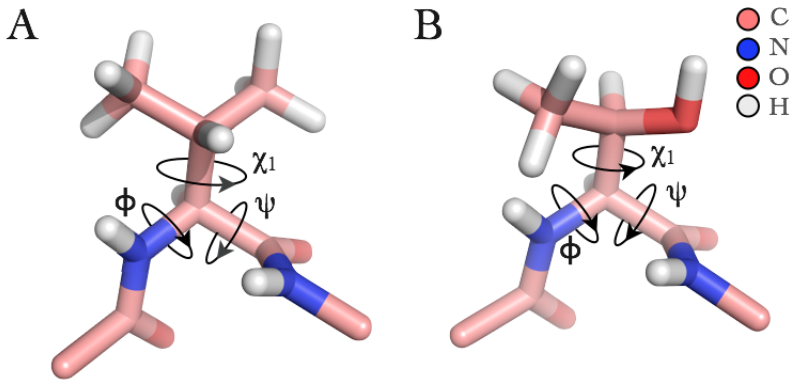

Figure 1: **Stick representation of (A) Val and (B) Thr dipeptide mimetics** Both Val and Thr are shown in an α-helix backbone conformation ($\phi = -57°$ defined by C'-N-C_α-C' and $\psi = -47°$ defined by N-C_α-C'-N). The values of the side-chain dihedral angle χ_1 (N–C_α–C_β–$C_{\gamma 1}$), 179.5° for Val and 117.7° for Thr, are indicated.

Figure S2

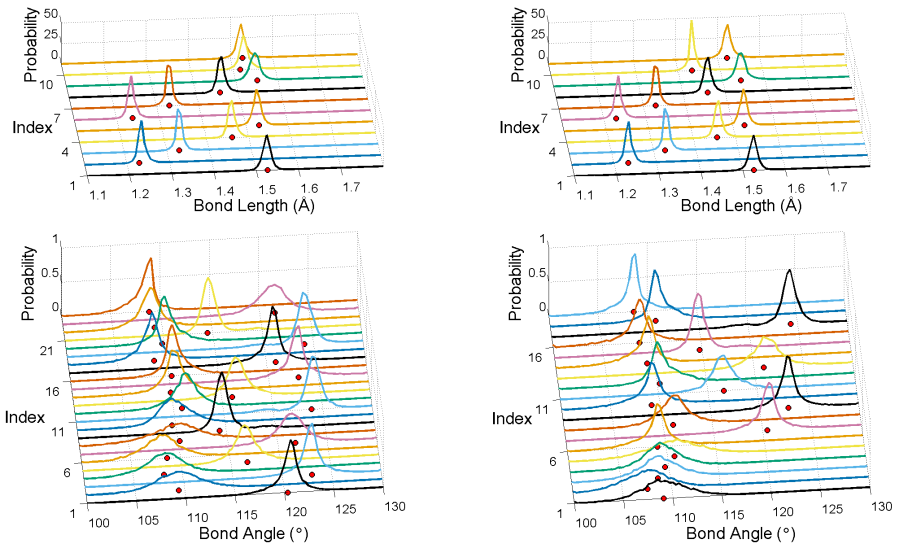

Figure 2: **Observed distributions of bond lengths and angles for Val and Thr** Plots of the observed probability distributions of all bond lengths (top) and bond angles (bottom) for Val (left) and Thr (right) from the Dunbrack database. Each of the 11 bond types (both Val and Thr), 24 bond angles for Val, and 19 bond angles for Thr are identified by indexes given in Tables 1, 2, 3 and 4. The red circles indicate the values of the bond lengths and angles used in our hard-sphere model for the dipeptide mimetics. The units of probability are Å^{-1} and deg^{-1} in the top and bottom panels, respectively.

Figure S3

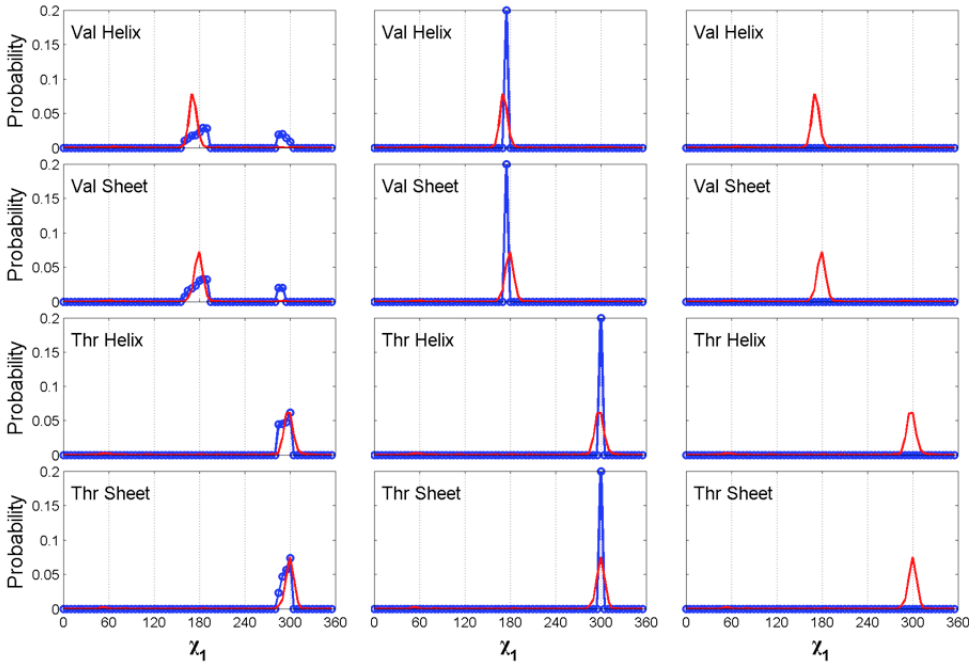

Figure 3:
Comparison of the probability distributions of the observed and calculated side-chain dihedral angles for Val and Thr using different sets of atom sizes Probability distributions of the side-chain dihedral angle χ_1 from the Dunbrack distribution (1) (red lines) are compared to predictions from our hard-sphere model (blue circles) for Val (α-helix and β-sheet) and Thr (α-helix and β-sheet) for the optimal atom sizes shown as star symbols in Fig.4 (middle, main text), the same atom sizes as those in the middle panel except the radius of Csp^3 is 1.35Å(left), and the same atom sizes a those in the middle panel except the radius of Csp^3 is 1.55Å(right).

Figure S4

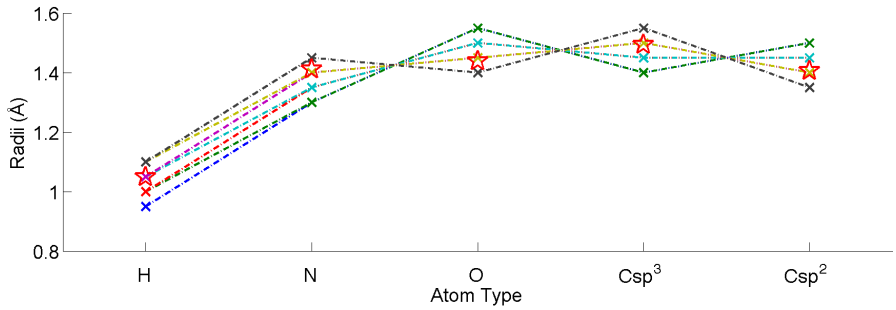

Figure 4:
The seven combinations (different line types and symbols) of five atom sizes that yield the smallest combined scores S_3 for both Thr and Val in the α-helix and β-sheet backbone configurations (*i.e.* all four scores, Thr-α-helix, Thr-β-sheet, Val-α-helix, and Val-β-sheet, are near the smallest threshold score $S_3^{\min}$). The star symbols indicate the mean radius for each atom type averaged over the seven combinations, which we selected as the optimal radii.

Figure S5

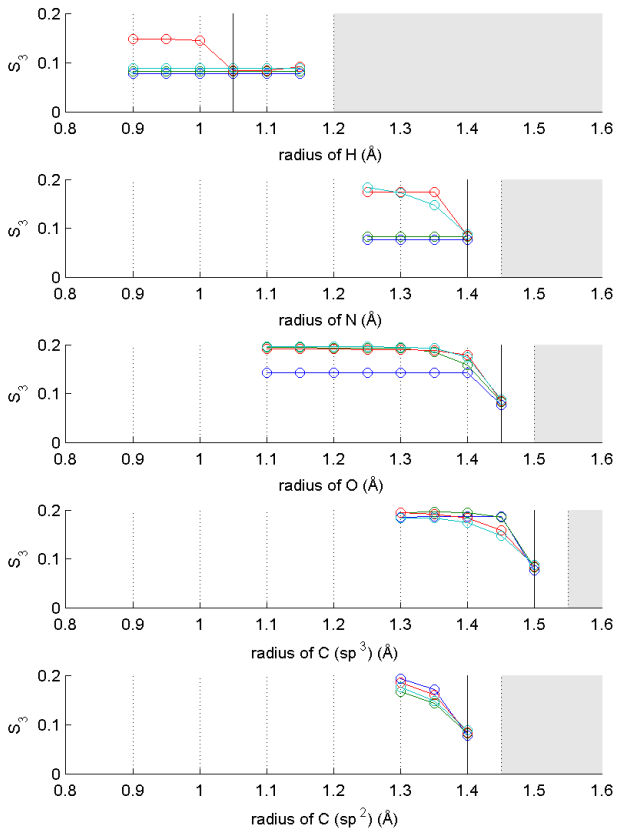

Figure 5: Sensitivity of the score S_3 for our predictions of the χ_1 distributions for Thr α-helix (red), Thr β-sheet (cyan), Val α-helix (blue), and Val β-sheet (green) to variations in the radius of H, N, O, C(sp^3), and C(sp^2) (from top to bottom). We vary each atom size individually, *e.g.* in the top panel we fix the sizes of N, O, C(sp^3), and C(sp^2) to the values given in Fig. 4 (solid vertical lines) and vary the size of H. The shaded gray region indicates atom size combinations for which there are no allowed configurations without atomic overlaps.

Figure S6

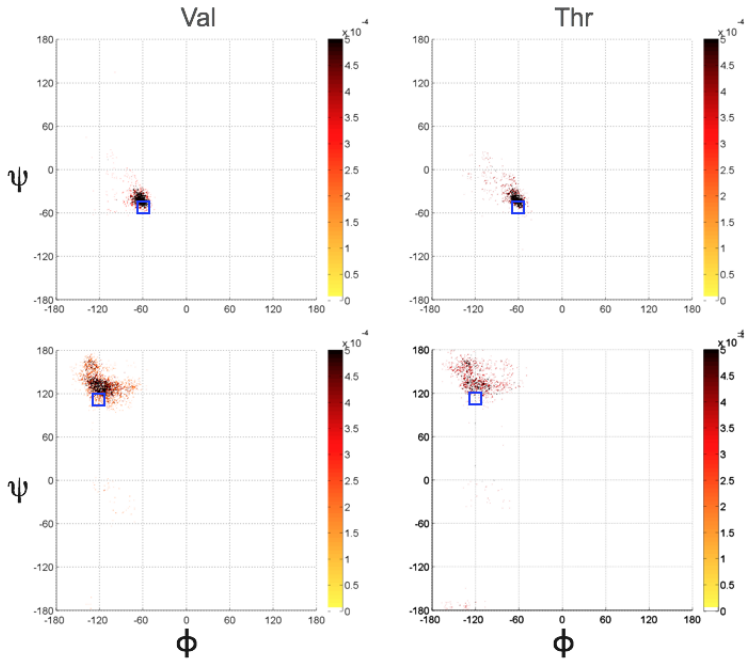

Figure 6:
Probability distributions for ϕ and ψ The probability distributions for the backbone dihedral angles ϕ and ψ from the Dunbrack database for Val (left) and Thr (right) in the α-helix (top row) and β-sheet (bottom row) conformations. The color scale from white to yellow to red to black indicates increasing probability. The boxes indicate ϕ and ψ angles that vary by $\pm 10^\circ$ from the canonical values for α-helix ($\phi = -57^\circ$, $\psi = -47^\circ$) (top row) and β-sheet ($\phi = -119^\circ$, $\psi = 113^\circ$) (bottom row).

Table S1

Table 1: Key for Fig. S2 (top-left). The bond associated with the Val dipeptide mimetic indexed from 1 to 11.

Index	Bond
1	$C_\alpha(i-1)$-C'$(i-1)$
2	C'$(i-1)$-O$(i-1)$
3	C'$(i-1)$-N(i)
4	N(i)-$C_\alpha(i)$
5	$C_\alpha(i)$-C'(i)
6	C'(i)-O(i)
7	C'(i)-N$(i+1)$
8	N$(i+1)$-$C_\alpha(i+1)$
9	$C_\alpha(i)$-$C_\beta(i)$
10	$C_\beta(i)$-$C_{\gamma_1}(i)$
11	$C_\beta(i)$-$C_{\gamma_2}(i)$

Table S2

Table 2: Key for Fig. S2 (bottom-left). The bond angles associated with the Val dipeptide mimetic indexed from 1 to 24.

Index	Bond Angle
1	$C_\alpha(i-1)$ -C'$(i-1)$ -O$(i-1)$
2	$H_{C_\alpha}(i)$ -$C_\alpha(i)$ -C'(i)
3	N(i) -C'$(i-1)$ -O$(i-1)$
4	$H_{C_\alpha}(i)$ -$C_\alpha(i)$ -N(i)
5	$C_\alpha(i-1)$ -C'$(i-1)$ -N(i)
6	$H_{C_\alpha}(i)$ -$C_\alpha(i)$ -$C_\beta(i)$
7	$C_\alpha(i)$ -N(i) -C'$(i-1)$
8	N(i) -$C_\alpha(i)$ -C'(i)
9	$C_\alpha(i)$ -N(i) -$H_N(i)$
10	$C_\beta(i)$ -$C_\alpha(i)$ -C'(i)
11	C'$(i-1)$ -N(i) -$H_N(i)$
12	N(i) -$C_\alpha(i)$ -$C_\beta(i)$
13	N(i) -C'(i) -$C_\alpha(i)$
14	$H_{C_{\gamma_1}}(i)$-$C_\beta(i)$ -$C_{\gamma_2}(i)$
15	O(i) -C'(i) -N(i)
16	$H_{C_{\gamma_1}}(i)$-$C_\beta(i)$ -$C_\alpha(i)$
17	$C_\alpha(i)$ -C'(i) -O(i)
18	$H_{C_{\gamma_1}}(i)$-$C_\beta(i)$ -$H_{C_\beta}(i)$
19	C'(i) -N$(i+1)$ -$H_N(i+1)$
20	$C_{\gamma_2}(i)$ -$C_\beta(i)$ -$C_\alpha(i)$
21	$H_N(i+1)$ -N$(i+1)$ -$C_\alpha(i+1)$
22	$C_{\gamma_2}(i)$ -$C_\beta(i)$ -$H_{C_\beta}(i)$
23	$C_\alpha(i+1)$ -N$(i+1)$ -C'(i)
24	$C_\alpha(i)$ -$C_\beta(i)$ -$H_{C_\beta}(i)$

Table S3

Table 3: Key for Fig. S2 (top-right). The bond associated with the Thr dipeptide mimetic indexed from 1 to 11.

Index	Bond
1	$C_\alpha(i-1)$-C'$(i-1)$
2	C'$(i-1)$-O$(i-1)$
3	C'$(i-1)$-N(i)
4	N(i)-$C_\alpha(i)$
5	$C_\alpha(i)$-C'(i)
6	C'(i)-O(i)
7	C'(i)-N$(i+1)$
8	N$(i+1)$-$C_\alpha(i+1)$
9	$C_\alpha(i)$-$C_\beta(i)$
10	$C_\beta(i)$-$O_{\gamma_1}(i)$
11	$C_\beta(i)$-$C_{\gamma_2}(i)$

Table S4

Table 4: Key for Fig. S2 (bottom-right). The bond angles associated with the Thr dipeptide mimetic indexed from 1 to 19.

Index	Bond Angle
1	$H_{C_\alpha}(i)$-$C_\alpha(i)$ -C'(i)
2	$H_{C_\alpha}(i)$-$C_\alpha(i)$ -N(i)
3	$H_{C_\alpha}(i)$-$C_\alpha(i)$ -$C_\beta(i)$
4	N(i)-$C_\alpha(i)$ -$C_\beta(i)$
5	N(i)-$C_\alpha(i)$ -C'(i)
6	$O_{\gamma_1}(i)$-$C_\beta(i)$-$C_{\gamma_2}(i)$
7	$C_\alpha(i-1)$-C'$(i-1)$-O$(i-1)$
8	$C_\beta(i)$-$C_\alpha(i)$-C'(i)
9	N(i)–C'$(i-1)$-O$(i-1)$
10	$O_{\gamma_1}(i)$-$C_\beta(i)$-$C_{\gamma_2}(i)$
11	$C_\alpha(i-1)$-C'$(i-1)$-N(i)
12	$O_{\gamma_1}(i)$-$C_\beta(i)$-$H_{C_\beta}(i)$
13	$C_\alpha(i)$-N(i)-C'$(i-1)$
14	$O_{\gamma_1}(i)$ -$C_\beta(i)$-$C_\alpha(i)$
15	$C_\alpha(i)$-N(i)-$H_N(i)$
16	$C_{\gamma_2}(i)$ -$C_\beta(i)$-$H_{C_\beta}(i)$
17	C'$(i-1)$-N(i)-$H_N(i)$
18	$C_{\gamma_2}(i)$ -$C_\beta(i)$-$C_\alpha(i)$
19	$C_\alpha(i)$ -$C_\beta(i)$-$H_{C_\beta}(i)$

References

1. Dunbrack R. L. and F. E. Cohen. 1997. Bayesian statistical analysis of protein side-chain rotamer preferences. *Protein Sci.* 6:1661–1681.